IV. DISCUSSION

In this paper the proposal by Mittleman,[5] to use the two-particle Bethe-Goldstone equation to describe electron scattering by an alkali atom, has been extended to a general theory of one-particle scattering by a many-particle system. The definition of net phase shift increments of successively higher orders makes it possible through a hierarchy of n-particle Bethe-Goldstone equations to obtain phase shifts of arbitrary accuracy.

A similar method has been shown to be practicable for calculation of the correlation energy of light atoms.[6,7] In addition to the evaluation and manipulation of large numbers of matrix elements of the atomic Hamiltonian for normalized atomic orbitals, for which the methods, developed in stationary-state calculations should suffice, there are special problems arising from the nature of the continuum orbital ϕ_k in scattering theory. Coulombic integrals must be evaluated in which the charge densities contain oscillatory as well as exponentially decreasing functions. In using the method outlined in Sec. III, a continuum integro-differential equation, Eq. (12), must be solved. However, since this equation has the same formal structure as the Hartree-Fock equations, considerable experience in the necessary numerical methods is available.

A very useful test of the practicability of the proposed method would be calculations of the phase shifts for low-energy elastic scattering of electrons by He and Ne atoms. Excellent calculations on He [11] and Ne [12] have recently been published, and the present method should be tested by its ability to refine or to systematize such work.

[11] J. Lawson, H. S. W. Massie, J. Wallace, and D. Wilkinson, Proc. Roy. Soc. (London) **A294**, 149 (1966).
[12] D. G. Thompson, Proc. Roy. Soc. (London) **A294**, 160 (1966).

PHYSICAL REVIEW VOLUME 156, NUMBER 1 5 APRIL 1967

Measurement of the Lamb Shift in the $n=4$ Level of He^+: RF Spectroscopy Using Time-Resolved Optical Detection*

L. L. HATFIELD†* AND R. H. HUGHES
Department of Physics, University of Arkansas, Fayetteville, Arkansas
(Received 21 November 1966)

A microwave measurement of the $4s_{1/2}$–$4p_{1/2}$ separation in He^+ has been obtained, using a method which involves time-resolved optical detection. Population changes induced by the microwaves in the $4s$ ($m=+\frac{1}{2}$) state are observed via intensity changes in the λ4686 Å ($n=4\rightarrow 3$) transition. The result of eleven measurements of the separation is $1766.0_0\pm 7.5$ MHz. The lifetime of the $4s_{1/2}$ state was measured to be $(1.3_6\pm 0.2_0)\times 10^{-8}$ sec.

I. INTRODUCTION

THE fine structure of the $n=4$ level in He^+ has been the subject of several experimental investigations. Series[1] performed a high-resolution optical study of the λ4686 Å radiation ($n=4\rightarrow 3$ transition in He^+) produced in a hollow-cathode discharge tube, and reported agreement with the theory except for a large shift of the $4^2P_{1/2}$ level downward from the predicted position.

A similar study by Herzberg[2] showed satisfactory agreement with the theory for all components of the λ4686 Å line.

Roesler and DeNoyer[3] investigated the helium hollow-cathode discharge and concluded that differential Doppler displacements of the spectral lines originating from the four $n=4$ levels could cause large shifts in the experimentally determined positions of the levels.

Roesler and Mack[4] studied the λ4686 Å radiation from a hollow-cathode discharge tube and reported over-all agreement between the experimentally determined positions of the components and the positions predicted by the theory, including quantum-electrodynamic corrections. The accuracy of these optical measurements was not sufficient to test the quantum electrodynamic theory to better than a few percent.

Lea, Leventhal, and Lamb[5] have reported the results of preliminary measurements on the $4^2S_{1/2}$–$4^2P_{1/2}$ and $4^2P_{3/2}$–$4^2P_{1/2}$ separations. Their method employs a dc electron beam to produce excited He^+ and a rf field to induce $4^2S_{1/2}$–$4^2P_{1/2}$ or $4^2P_{3/2}$–$4^2S_{1/2}$ transitions which are observed as intensity variations in the λ1215 Å ($n=4\rightarrow 2$) radiation. Their result for the Lamb shift is 1765±20 MHz, which agrees with the theoretical value of 1769 MHz obtained from the work of Erickson.[6]

* Supported by the National Science Foundation.
† Present address: Physics Department, Rice University, Houston, Texas.
[1] G. W. Series, Proc. Roy. Soc. (London) **A226**, 377 (1954).
[2] G. Herzberg, Z. Physik **146**, 269 (1956).
[3] F. L. Roesler and L. DeNoyer, Phys. Letters **12**, 396 (1964).
[4] F. L. Roesler and J. E. Mack, Phys. Rev. **135**, A58 (1964).
[5] K. R. Lea, M. Leventhal, and W. E. Lamb, Jr., Phys. Rev. Letters **16**, 163 (1966).
[6] G. W. Erickson, Phys. Rev. Letters **15**, 338 (1965).

TABLE I. Computed lifetime of $n=4$ He^+ states (Ref. 2).

Level	Mean lifetime (10^{-8} sec)
4^2S	1.4154
4^2P	0.07687
4^2D	0.2258
4^2F	0.4531

The method of rf spectroscopy using time-resolved optical detection, which is employed in this measurement of the $4s_{1/2}$–$4p_{1/2}$ separation in He^+, is based on the sampling technique of Pendleton and Hughes[7] for the direct measurement of atomic lifetimes. In these lifetime measurements, a gated beam of electrons of controlled energy is used to excite target gas atoms. When the electron beam is gated off, the atoms undergo radiative decay in an approximately field-free region. The decay is monitored by a dc-operated photomultiplier and a sampling oscilloscope.

In principle, rf spectroscopy using time resolution can be employed to determine the separation of any two close-lying states having different lifetimes. In the case of measuring the $4^2S_{1/2}$–$4^2P_{1/2}$ separation in He^+, advantage can be taken of the fact that the $4s$ lifetime (Table I) is considerably longer than the lifetime of any other $n=4$ state that might be populated by the excitation pulse. Radiative decay of these states can be observed through the λ4686 Å ($n=4\rightarrow 3$) complex. The oscilloscope can be set to sample the photomultiplier output at a time after cutoff of the excitation pulse when only the $4s\rightarrow 3p$ radiation is present. The $4s$ decay is then effectively isolated, and standard rf methods can be employed (see Appendix).

In addition to the advantage of a built-in method for producing population differences, there may be a decided advantage in being able to make the measurements when the excitation pulse is off. This is valuable when the excitation pulse can produce appreciable perturbation of the involved levels, such as the Stark mixing due to the electric fields from the space charge of a high-density electron beam.

The experiment was performed using 300-eV electron impact as the excitation mechanism which preferentially populates the $4s$ state.[8] Since the excitation mechanism provides the population difference, the basic appeal of time resolution in the actual experiment is not in the ability to produce population differences, but in the fact that the measurement can be performed when the radiating atoms are in an environment free from the fields produced by the electron-beam space charge. (It should be pointed out, however, that the rf is gated on during the on time of the electron beam in this particular experiment.)

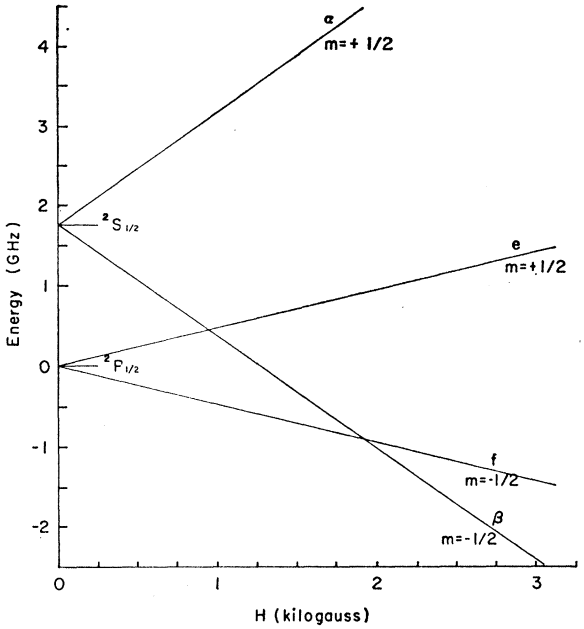

FIG. 1. Zeeman splitting of the $4^2S_{1/2}$ and $4^2P_{1/2}$ levels of He^+.

As with most experiments of this type, the procedure is to fix the rf frequency and to shift the Zeeman states in and out of resonance by changing the magnetic field in the interaction region.

The Zeeman splitting of the $4^2S_{1/2}$ and $4^2P_{1/2}$ levels is shown in Fig. 1. The zero-field separation is taken as the theoretical value 1768 MHz.[9] The theory of the Zeeman effects gives, for the energies of the $\alpha\beta$ and ef components[10]:

$$E_{\alpha\beta}=S\pm\tfrac{1}{2}g_s\mu_0H,$$

$$E_{ef}=\tfrac{1}{2}\Delta E\pm\tfrac{1}{2}g_L\mu_0H-\tfrac{1}{2}[(\Delta E)^2\pm\tfrac{2}{3}\Delta Eg\mu_0H+(g\mu_0H)^2]^{1/2},$$

where S is the Lamb shift, ΔE is the $4^2P_{3/2}$–$4^2P_{1/2}$ interval, g_s is the spin-dependent part of the Landé g factor, g_L is the orbital-angular-momentum–dependent

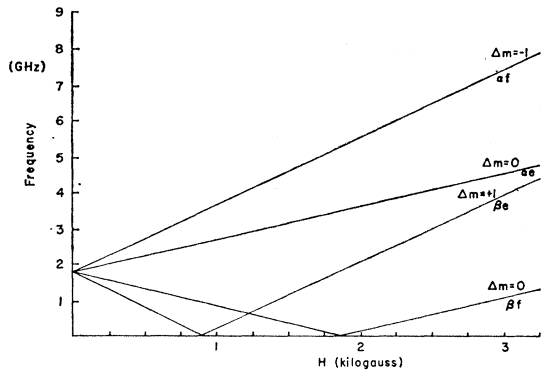

FIG. 2. Transition frequency versus magnetic field.

[7] W. R. Pendleton and R. H. Hughes, Phys. Rev. **138**, A683 (1965).
[8] E. T. P. Lee and C. C. Lin, Phys. Rev. **138**, A301 (1965).
[9] J. D. Garcia and J. E. Mack, J. Opt. Soc. Am. **55**, 654 (1965).
[10] W. E. Lamb, Jr., and T. M. Sanders, Jr., Phys. Rev. **119**, 1901 (1960).

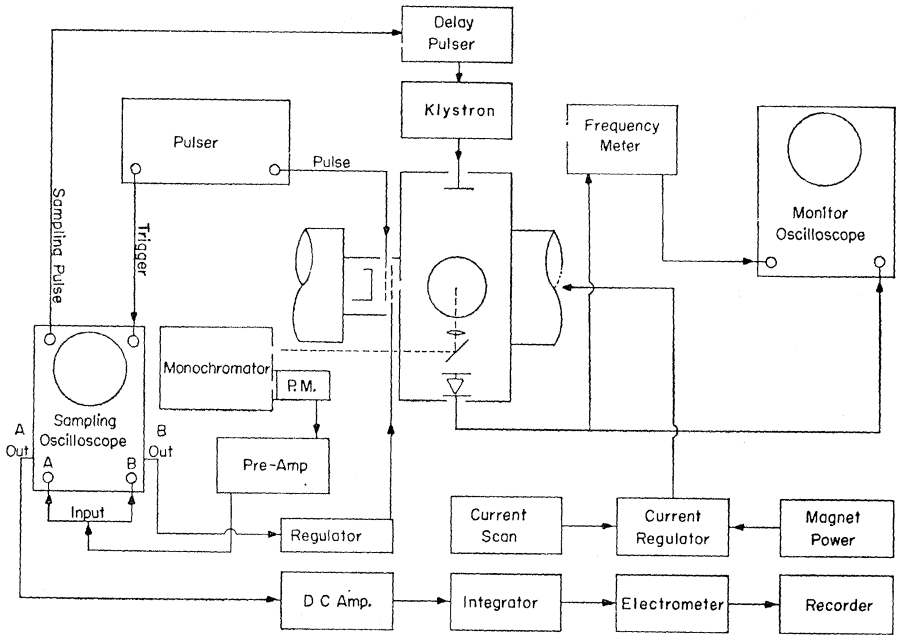

FIG. 3. Block diagram of the experimental apparatus.

part of the Landé g factor, and $g=g_s-g_L$. The frequency of the allowed electric-dipole transitions is diagrammed in Fig. 2 as a function of magnetic field. For the αe transition, the Lamb shift is given by

$$S=\nu-\frac{1}{2}\frac{\mu_0}{h}gH+\frac{1}{2}\frac{\Delta E}{h}-\frac{1}{2}\left[\left(\frac{\Delta E}{h}\right)^2+\frac{2}{3}\frac{\Delta E}{h}\frac{\mu_0}{h}gH+\left(\frac{\mu_0}{h}gH\right)^2\right]^{1/2},$$

where

$$\nu=(E_\alpha-E_e)/h.$$

II. EXPERIMENTAL APPARATUS

A. Excitation System

The interaction chamber is a 6-in.-long piece of RG 75/U bronze waveguide. The electron-gun housing is attached to the side of the waveguide and the electron beam enters the interaction region through a slot in the wall. The viewing port is above the interaction region. The ends of the chamber are sealed with aluminum flanges with glass windows which transmit the rf radiation. The entire assembly is placed in the magnet gap.

The electron gun is a 6DW5 power pentode with the glass envelope, base, and plate structure removed. The remaining assembly is spot welded to leads introduced into the chamber through vacuum feed-throughs.

The chamber is at ground potential and the cathode is made 300 V negative with respect to the chamber. This determines the energy of the electron beam. The first grid is biased to cut off the electron beam, and the second grid is made positive relative to the cathode as an aid in focusing the beam.

The pulser shown in Fig. 3 is a Dumont 404B which produces a 50-V pulse when connected to a 50-Ω load. This pulse is applied to the first grid of the electron gun to control the electron beam. The electron-beam pulse was studied with a Faraday cup inserted from one end of the chamber. With a pulse width of 50 nsec and a repetition rate of 10^4 pulses/sec, pulses of up to 40 mA were observed. The rise and fall times (10 to 90%) of the pulse were about 7.7 nsec. During data runs, the Faraday cup cannot be used, because of the large electrical discontinuity it presents to the rf field. During a run, the size of the beam pulse is inferred from the size of the cathode current pulse.

The vacuum manifold is pumped by an oil diffusion pump with a liquid-air-cooled trap mounted above it. An ionization gauge is used to monitor the high vacuum necessary for activation of the electron-gun cathode and a Pirani gauge is used to measure the operating pressure, which is about 0.1 Torr.

Helium is introduced into the vacuum manifold through a variable leak and a liquid-air-cooled charcoal trap. This trap absorbs impurity gases generated by the hot electron-gun cathode.

B. Microwave System

The amount of rf power needed can easily be estimated. From the quantum theory of radiation, the number of transitions induced per sec, W, is given by

$$W=\frac{2\pi\gamma S_0|(|\mathbf{e}\cdot\mathbf{r}|)|^2}{c\hbar^2[(\omega-\omega_0)^2+\frac{1}{4}\gamma^2]},$$

where $\gamma=1/\tau_s+1/\tau_p$ is the radiation damping constant, τ_s and τ_p are the radiative lifetimes of the 4_s and 4_p states, respectively, S_0 is the energy flux density of

radiation having angular frequency ω and electric vector parallel to the unit vector $\mathbf{e}$, ω_0 is the resonance angular frequency, and $(|\mathbf{r}|)$ is the matrix element of the coordinate vector for the $4^2S_{1/2}$–$4^2P_{1/2}$ transition. For a transition which requires $\mathbf{e}$ to be along $\mathbf{z}$,[11] the axis of quantization,

$$|(|\mathbf{e}\cdot\mathbf{r}|)|^2=|(|z|)|^2=15a_0^2,$$

where a_0 is the radius of the first Bohr orbit. For $W=1/\tau_s$ and $\omega=\omega_0$, the energy flux density is $S_0=132$ mW/cm^2. With our waveguide, the power requirement is about 3.8 W. (During data runs, the power used was of the order of 1 W.)

The microwave oscillator is a General Radio 1220-A unit oscillator. This unit uses a 6043 klystron to produce 65 mW at 3260 MHz. The oscillator includes modulation circuits which are used to switch the rf. The output of the oscillator is connected through an adjustable attenuator to a 2K35 klystron amplifier which will produce about 25 W at 3260 MHz with a 25-mW input power.

The output of the 2K35 amplifier is connected to a waveguide adapter bolted to one end of the interaction chamber. A termination is bolted to the other end to eliminate reflection. Part of the power absorbed by the termination is applied to a microwave detector whose output is displayed by a monitor oscilloscope to determine the microwave pulse shape, size, and timing.

A small amount of the rf power absorbed by the termination is directed to a TS 186 A/UP heterodyne frequency meter. Calibration of the heterodyne oscillator is accomplished with a crystal controlled oscillator whose frequency is compared with the 10 MHz carrier of radio station WWV. The microwave signal and the heterodyne oscillator output are mixed, and the beat frequency is displayed by the monitor oscilloscope. The accuracy of the microwave frequency measurement is 0.01%.

C. Magnetic Field

The magnetic field in the interaction region is produced by an Alpha AL7500 electromagnet with 4-in.-diam pole faces and a 2-in. gap. This magnet produces up to 2500 G with a gradient of less than 0.1 G over a 2-cm-diam region in the center of the pole face. The interaction region is limited to this dimension.

The magnet current is regulated by an Alpha 7500R series current regulator. The maximum current drift over a 24-h period is 0.1% and the resolution is 0.04%. The magnetic field was calibrated by observing the proton NMR in a water sample substituted in the interaction region. A maximum current setting was selected to define a hysteresis loop and the proton NMR observed for 30 regulator dial settings on each side of the loop from 800 to 2500 G. From a series of six independent measurements over a period of one year, the resettability is ±3 G at 2000 G with the size of the uncertainty proportional to the size of the field.

During a data run, the magnetic field is scanned by turning the regulator dial with a synchronous motor.

D. Detection System

Radiation from the interaction region is focused by a lens and mirror system on the entrance slit of a Jarrell-Ash 0.5-m Ebert monochromator having a spectral slit width of 12 Å. This slit width was required to isolate the λ4686 Å line from the λ4713 Å He I line which was many times stronger than λ4686 Å when the magnetic field was turned on. The λ4686 Å radiation is selected and focused on a photomultiplier in a shielded housing. The response time of the detection system was measured by using a test light pulser. An EMI 6256B photomultiplier with a response time of about 12 nsec (10 to 90%) is used in the Lamb-shift measurement. The measurement of the decay time of the atoms required the use of an Amperex 56AVP which has a 2-nsec response time, but which produces a lower signal-to-noise ratio than the EMI tube. In both cases, the high-voltage supply and the last five dynodes of the photomultiplier are rf decoupled to eliminate feedback effects. The anode of the photomultiplier is terminated with a 50-Ω resistor to match the input impedance of the preamplifier.

The photomultiplier-current pulses are preamplified by a Keithley 104 wide-band amplifier, which has a 3-nsec response time and a gain of 100. The output of the last stage is connected to both channels of the sampling oscilloscope.

The sampling oscilloscope is a Lumatron model 120 which has two identical vertical channels operated by a single horizontal unit. The response time of the vertical units is 0.35 nsec. This oscilloscope has been modified to make the vertical units sample alternately.

The pulser which drives the electron gun triggers the oscilloscope at a preset time before each electron-beam pulse. A sample is taken at a time after the trigger pulse which is determined by the oscilloscope control settings.

The radiation-decay curve is obtained by advancing the sample time by a fixed amount after each light pulse and recording the oscilloscope output on a strip chart. A smoothing circuit in the oscilloscope averages successive samples to reduce random fluctuations. A detailed discussion of the display of the decay curve by this equivalent is available elsewhere.[7]

In the Lamb-shift measurement, the oscilloscope is set to sample the photomultiplier-output pulse at about 20 nsec, after the electron beam has been gated off. The photomultiplier output is alternately switched, so that oscilloscope channel A samples every other light pulse, while channel B samples the remainder. A pulse which is synchronous with the channel-B sampling pulse is

[11] H. A. Bethe and E. E. Salpeter, *Quantum Mechanics of One- and Two-Electron Atoms* (Academic Press Inc., New York, 1957), p. 254.

electronically delayed and applied to the microwave oscillator to gate the rf on during the cycle monitored by channel A (see Fig. 3). With this alternate-sampling arrangement, channel A samples the photomultiplier signal when the rf is on. The rf is gated on for channel A prior to turning on the electron beam, and is gated off after the electron beam is turned off at times which ensure that the entire atomic-excitation and atomic-decay cycle takes place in a uniform rf field. Channel B monitors the cycle when the rf is off.

A current-regulating device is used to ensure that small fluctuations in the electron beam during the data runs will not affect the data. The output of channel B is amplified by a Philbrick U.S.A.-3 operational amplifier with a gain of 800. The output of the amplifier is in series with the power supply for the second grid of the electron gun. A negative feedback loop is produced which maintains a constant level for channel B (the rf-off channel).

The output for channel A is amplified by a Philbrick U.S.A.-3 operational amplifier adjusted for suitable gain and bandwidth. This amplifier output is applied to an RC integrator, the output of which is measured by a General Radio 1230-A electrometer. The electrometer drives a recorder which traces the resonance curve.

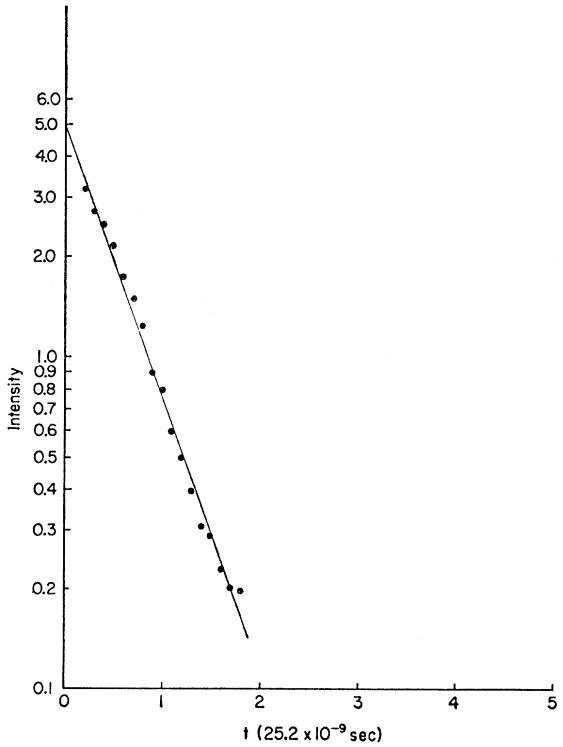

FIG. 4. Semilog plot of λ4686 Å decay. This resolves into a single decay which is attributed to the 4*s* decay.

III. RESULTS

A. Lifetime

The experimental result for the lifetime of the 4*s* state of He^+ is $(1.3_6\pm0.2_0)\times10^{-8}$ sec. This is the average of 13 independent measurements. Figure 4 shows a semilog plot of the λ4686 Å decay.

The response time of the sampling system using the Amperex-56AVP photomultiplier tube is 3.08 nsec. However, the electron-beam pulse-fall time is about 7.7 nsec. The over-all response of the system is then about 8.3 nsec. This does not affect the measurement of the 4*s* lifetime, but any shorter-lived components would appear as an approximately 8.3-nsec contribution to the lifetime. None of the data showed any shorter-lived components, which confirms the heavy *s*-state population estimates of Lee and Lin.[8] Contributions by the short-lived states must be less than 15% to avoid detection.

B. The Lamb Shift

Figure 5 shows a typical recording of the resonance curve. The Lamb shift is determined from the αe resonance by finding the center of the absorption curve. Each measurement is the averaged result of a pair of curves taken in opposite directions of change of the magnetic field. One curve represents about 60 min of operation. The integration time is 1.5 min (10 to 90%). The center of the curve is located by plotting the midpoints of about 30 equally spaced horizontal sections of the curve. The line drawn through these points is vertical if the curve is symmetrical. All of the curves used in the measurement were symmetric.

The measured value of the Lamb shift is obtained by inserting the magnetic field strength corresponding to the center line and the measured value of the rf frequency into the equation for S in Sec. I.

The averaged result of 11 pairs of curves is $1766._0$ MHz with an rms precision of $6._4$ MHz. The experimental uncertainty is estimated to be ±7.5 MHz by taking the sum of the following estimated uncertainties: rf frequency—±0.3 MHz, magnetic field—±3.2 MHz, line-center measurement—±4 MHz.

The value of ΔE, the $4^2P_{3/2}$–$4^2P_{1/2}$ interval, is taken from the tables of Garcia and Mack.[9] The value for g_s is[12]

$$g_s=2(1+a),$$

where

$$a=1.159622\times10^{-3}\pm27\times10^{-9}.$$

All other numerical values are taken from the 1955 Table of Atomic Constants.[13]

The theoretical value for the $4^2S_{1/2}$–$4^2P_{1/2}$ interval in He^+ is 1768.2±0.6 MHz, from the tables of Garcia and Mack.[9,14]

---

[12] D. T. Wilkinson and H. R. Crane, Phys. Rev. **130**, 852 (1963).
[13] E. R. Cohen, J. W. M. Dumond, T. W. Layton, and J. S. Rollett, Rev. Mod. Phys. **27**, 363 (1955).
[14] The uncertainty quoted was verified by J. D. Garcia (private communication).

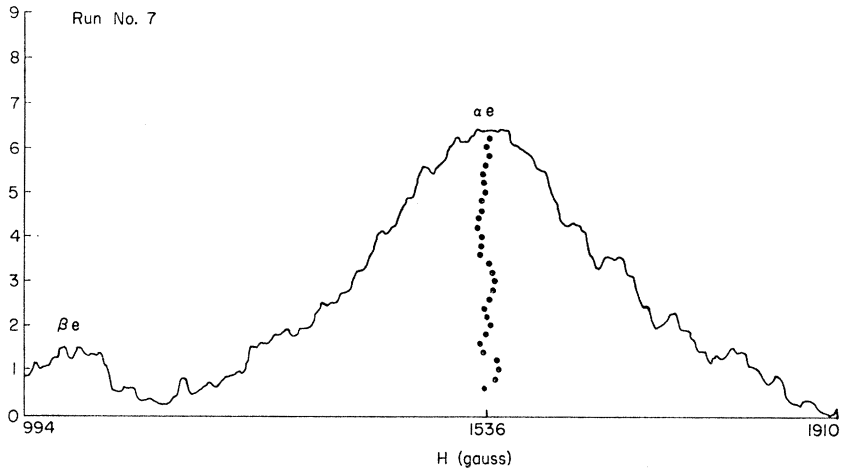

FIG. 5. Typical recording showing the αe resonance line and the βe zero crossing.

IV. DISCUSSION

It would seem appropriate to comment on the βe zero crossing resonance curve that appears in Fig. 5. Since the signal is essentially the difference between rf off and rf on, it is evident that the rf produces an electric perturbation which Stark mixes these states when the energy difference between the states is small.

In principle, the βe resonance could be used for a further measurement of the $4s_{1/2}$–$4p_{1/2}$ separation. However, this resonance curve is instrumentally skewed. The electron-beam focus changes radically when the magnetic field is below 900 G. This produces a large intensity fluctuation which cannot be properly compensated for by the electron-beam regulating system.

The mere presence of the βe resonance places a generous upper limit on the magnitude of the Stark effect existing in the chamber when the rf is off. If the electric fields existing in the chamber when the rf is off were sufficient to produce full Stark mixing of these levels, then no βe crossing signal would be possible.

The perturbation required to fully mix β and e at the crossing can be calculated. Bethe and Salpeter[15] show that at the "critical field" required to produce full mixing, $f_{\beta e}^2=\beta_-^2$, where $f_{\beta e}=(\beta|e\mathbf{E}\cdot\mathbf{r}|e)$, is the Stark matrix element connecting the two states and $\beta_-=\frac{1}{2}(1/\tau_p-1/\tau_s)$. In frequency units, $\beta_-=49$ MHz. If the x, y, and z components of the electronic field $\mathbf{E}$ are equal, then[16]

$$f_{\beta e}^2=f_{\alpha f}^2=2f_{\alpha e}^2=2f_{\beta f}^2.$$

We now estimate the expected Stark effect of such a "critical" electric field on the energy difference between α and e at 1550 G, which is near the maximum on the αe resonance shown in Fig. 5. The energy differences for the states connected by the Stark effect are: $\omega_{\alpha e}=3260$ MHz, $\omega_{\alpha f}=4670$ MHz, and $\omega_{\beta e}=-1120$ MHz. At this magnetic field, the effect of the $p_{3/2}$ levels is neglected because of the large energy differences.

From the second-order Stark effect, state α is shifted by

$$\Delta E_\alpha=f_{\alpha e}^2/\omega_{\alpha e}+f_{\alpha f}^2/\omega_{\alpha f}=+0.87\text{ MHz},$$

and state e is shifted by

$$\Delta E_e=f_{\beta\iota}^2/\omega_{\beta e}+f_{\alpha e}^2/\omega_{\alpha e}=+1.79\text{ MHz}.$$

The net change in the interval E_α–E_e is -0.92 MHz.

Since, undoubtedly, $f_{\beta e}^2<\beta_-^2$, the Stark effect on the measurement around the maximum in the αe resonance is negligible. Since the resonance curve is symmetric, the Stark effect is assumed to be negligible elsewhere (within the accuracy of the experiment).

No study of the αe resonance line shape was attempted. The natural width of the curve at half-maximum is given by

$$\Delta\nu=\frac{1}{2\pi}(1/\tau_p+1/\tau_s)=218\text{ MHz},$$

or, expressed in terms of the magnetic field, the natural width is 234 G. The average half-width as measured from the data curves is about 210 G, but since the limits of uncertainty for a measurement at a single point on a curve are about ±25 G, no disagreement with theory can be claimed.

ACKNOWLEDGMENTS

The authors wish to thank Dr. S. M. Day for his valuable discussion of many aspects of the experiment. We also thank Albert Filippelli, who assisted in the data taking, and Walter Yancy, who constructed part of the equipment.

APPENDIX

To illustrate the possible advantage of rf spectroscopy using time resolution, we take the hypothetical

[15] Reference 11, p. 289.

[16] See E. U. Condon and G. H. Shortley, *The Theory of Atomic Spectra* (Cambridge University Press, London, 1935), p. 63, Eq. (11).

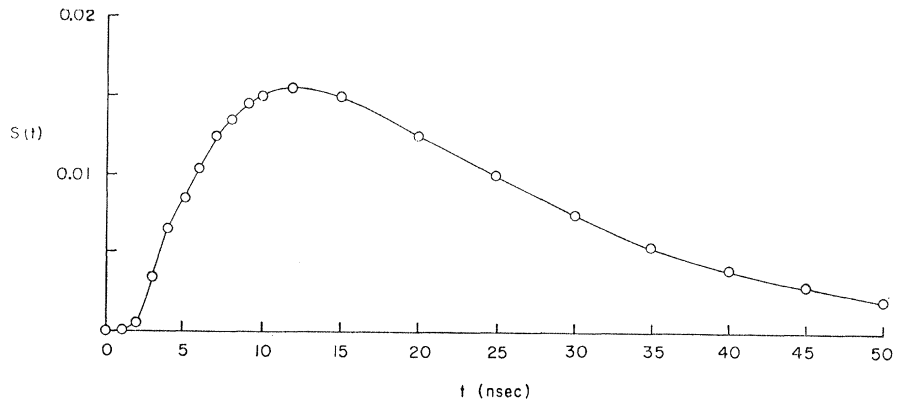

FIG. 6. Signal (see text) versus time after electron-beam cutoff.

case of measuring the $4^2S_{1/2}$–$4^2P_{1/2}$ separation in He^+ by detecting intensity changes in the λ4686 Å line when the populating mechanism produces equal equilibrium populations in the $4^2S_{1/2}$ and $4^2P_{1/2}$ states.

In writing the rate equations for the population of the $4s_{1/2}$ and $4p_{1/2}$ states, in this example, it is assumed that: (1) The population mechanism is gated on for a time sufficiently long to ensure that equilibrium has been established, with all magnetic substates populated equally prior to the excitation mechanism being turned off at $t=0$; (2) secondary population, such as cascade, is negligible; (3) the rf, tuned to resonance, produces W transitions per sec between a single pair of states, such as $m=+\frac{1}{2} \leftrightarrow m=+\frac{1}{2}$.

While the excitation pulse is on ($t<0$) and the rf off, we have, for the pair of states,

$$\dot{n}_s=-n_s/\tau_s+r_s, \tag{A1}$$

$$\dot{n}_p=-n_p/\tau_p+r_p, \tag{A2}$$

where n_s and τ_s are the atom density and field-free lifetime, respectively, of the $4s$ state; n_p and τ_p are the atom density and field-free lifetime, respectively, of the $4p$ state; r_s and r_p are the rate of populating the s state and the p state, respectively.

While the excitation pulse is on ($t<0$) and the rf is on,

$$\dot{n}_s=-n_s/\tau_s+r_s+W(n_p-n_s), \tag{A3}$$

$$\dot{n}_p=-n_p/\tau_p+r_p+W(n_s-n_p). \tag{A4}$$

After the excitation pulse is turned off ($t>0$), the rate equations for rf off and rf on are Eqs. (A1) and (A2), and (A3) and (A4), respectively, with $r_p=r_s=0$.

For $t>0$ and $r_s=r_p=0$, the solutions to (A1) and (A2) are

$$n_s^0=n_{s0}e^{-t/\tau_s}, \tag{A5}$$

$$n_p^0=n_{p0}e^{-t/\tau_p}. \tag{A6}$$

For $t>0$ and $r_s=r_p=0$, the solutions to (A3) and (A4) are

$$n_s=C_1\exp(m_+t)+C_2\exp(m_-t), \tag{A7}$$

$$n_p=C_3\exp(m_+t)+C_4\exp(m_-t), \tag{A8}$$

where $m_\pm=-\frac{1}{2}(a+b)\pm\frac{1}{2}[(a-b)^2+(2W)^2]^{1/2}$, $a=1/\tau_s+W$, and $b=1/\tau_p+W$.

Using the boundary conditions at $t=0$, $n_s=n_p=n_0$, thus $n_{s0}=n_{p0}=n_0$;

$$C_1=-n_0(1/\tau_s+m_-)(m_+-m_-)^{-1},$$
$$C_2=n_0(1/\tau_s+m_+)(m_+-m_-)^{-1},$$
$$C_3=-n_0(1/\tau_p+m_-)(m_+-m_-)^{-1},$$
$$C_4=n_0(1/\tau_p+m_+)(m_+-m_-)^{-1}.$$

The difference signal Δ, which is the intensity of the λ4686 Å line with the rf off minus the intensity with the rf on for $t>0$, is

$$\Delta(t)=K[(n_s^0-n_s)A_{4s\to3p}+(n_p^0-n_p)(A_{4p\to3s}+A_{4p\to3d})],$$

where K is a constant, n_s^0, n_p^0 and n_s, n_p are the atom densities with the rf off [Eqs. (A5) and (A6)] and rf on [Eqs. (A7) and (A8)], respectively, and the A's are the indicated spontaneous-transition probabilities.

We arbitrarily define a signal $I_0=K2n_0[A_{4s\to3p}+3(A_{4p\to3s}+A_{4p\to3d})]$ which effectively is the light signal at $t=0$ under the assumption of a statistical population of the p states and negligible population of the $4f$ and $4d$ states. We further define a parameter

$$S(t)=\Delta(t)/I_0.$$

In Fig. 6 we plot $S(t)$, using $W=1/\tau_s$. Since $n_s=n_p$ at excitation equilibrium, a rf measurement using continuous excitation would be impossible. However, using time resolution and measuring the signal at some time $t>0$ after excitation cutoff, $S(t)\neq0$.